DOI: 10.1002/ejoc.200900848

A Novel Diameter-Selective Functionalization of SWCNTs with Lithium Alkynylides

Benjamin Gebhardt,[a] Ralf Graupner,[b] Frank Hauke,[a] and Andreas Hirsch*[a]

Keywords: Nanotubes / Carbon / Alkynes / Raman spectroscopy / Nucleophilic addition

Covalent functionalization by addition to the sidewalls of single-walled carbon nanotubes (SWCNTs) is one of the most important methods for the derivatization of carbon nanotubes. The nucleophilic addition of organometallic reagents (carbon- and nitrogen-based carbanions) has recently become a widely used tool for the introduction of functional moieties onto the surface of this new carbon allotrope. The extension of this concept by the successful nucleophilic addition of in situ generated lithium acetylides to the SWCNT scaffold is presented herein. The chemically derivatized SWCNTs have been characterized in detail by TGA/MS, Raman, UV/Vis/NIR and fluorescence spectroscopy. On the basis of a detailed examination of the signals in the radial breathing-mode region of the Raman spectra, the preferred functionalization of smaller-diameter tubes has been clearly demonstrated.

Introduction

After their accidental discovery in the course of fullerene chemistry in 1991,[1] carbon nanotubes (CNTs) have become an extensively studied class of compounds due to their outstanding electronic and mechanical properties.[2,3] In this regard, the covalent sidewall functionalization of single-walled carbon nanotubes (SWCNTs) has become an important topic of research as it allows tuning of their solubility and processability, which is a key factor for their practical applications as new materials.[4–9] However, the polydispersity of as-prepared SWNCTs formed of mixtures of metallic and semiconducting species with different diameters and helicities represents a major problem, hampering their entry to nanoworld applications, for example, in the field of molecular electronics. One possible approach to overcoming this problem is the selective chemical addressability of specific types of tubes, for example, semiconducting versus metallic or small- versus large-diameter SWCNTs. Once a specific family of tubes has undergone preferred side-wall functionalization it might be separated from other tubes on the basis of their increased solubility.[10] The electronic properties may be restored upon subsequent thermal cleavage of the addends.[11] To tap the full potential of selective covalent sidewall functionalization, a set of derivatization sequences with gradual different reactivities is necessary. Although the reactivity of SWCNTs towards addition reactions is significantly lower than that of many other conjugated π-systems, including the more highly strained fullerenes, a large number of functionalization methods have been disclosed already, for example, fluorination,[12–14] cycloaddition reactions,[15–18] alkali-metal-based reductions followed by reaction with electrophiles,[19–22] Friedel–Crafts acylation[22] as well as the addition of diazonium compounds,[23–26] radicals[27–32] and organometallic reagents.[33–38] Some of these reactions have shown a preferred reactivity towards metallic nanotubes[25,37] or towards smaller-diameter species.[21,36,37,39,40]

Recently, a number of first approaches towards realizing this goal of a selective functionalization of metallic SWCNTs have been elaborated for diazonium reagents,[25,36,41,42] and the preferred reactivity towards metallic tubes for the nucleophilic addition of organometallic reagents has also been reported by our group.[36,37]

In this paper we report a nucleophilic addition sequence using a novel nucleophile; SWCNTs react with in situ generated lithium acetylides, leading to the direct covalent attachment of the organic moiety to the sidewalls of HiPCO® SWCNTs. The reagents used herein are less potent bases and weaker nucleophiles than, for example, alkyllithium and Grignard reagents or lithium amides, which have recently been used in our group for the direct and selective nucleophilic derivatization of SWCNTs.[21,36–40] In general, less reactive species undergo reactions in a more selective way, and based on this rationale it seems reasonable that lithium acetylides could exhibit a higher selectivity with respect to the addition to SWCNTs. The present study addresses this question for the first time. Conceptually, deprotonation of a terminal alkyne with *n*-butyllithium generates

[a] Department of Chemistry and Pharmacy and Institute of Advanced Materials and Processes (ZMP), Friedrich Alexander University of Erlangen-Nürnberg,
91054 Erlangen, Germany
Fax: +49-9131-8526864
E-mail: Hirsch@chemie.uni-erlangen.de
[b] Technical Physics, Friedrich Alexander Universität of Erlangen-Nürnberg
91058 Erlangen, Germany
Supporting information for this article is available on the WWW under http://dx.doi.org/10.1002/ejoc.200900848.

a terminal acetylide functionality, which subsequently should be able to attack the conjugated π-system of SWCNTs. As in the case of, for example, $(n\text{-butyl})_n$-SWCNT the resulting intermediate $(\text{alkyne})_n$-SWCNT^{n-} species should be able to undergo reoxidation by oxygen[36] to yield the final $(\text{alkyne})_n$-SWCNT adducts. Herein we demonstrate that acetylide anions are potent nucleophiles and that the corresponding alkyne SWCNT derivatives exhibit an improved dispersibility in organic solvents such as THF. We also show that the addition of alkynylides proceeds preferably on small-diameter carbon nanotubes and that aliphatic acetylides exhibit a more pronounced reactivity than their aromatic analogues due to their higher nucleophilicity.

Results and Discussion

To exploit the potential of lithium acetylides in the nucleophilic attack of the π-system of SWCNTs, several reaction sequences were carried out by varying the nature of the terminal alkyne [pentyne (**1**), decyne (**2**), phenylacetylene (**3**), *m*-tolylacetylene (**4**)], solvent [*o*-dichlorobenzene (*o*-DCB), *o*-xylene, diglyme] and temperature (80, 120, 160 °C).

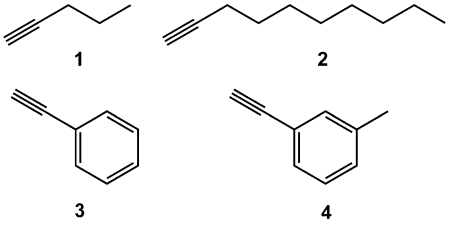

The corresponding lithium acetylide of pentyne (**1**) was prepared in situ by deprotonation with 0.9 equiv. of *n*-butyllithium in THF (Scheme 1). Single-walled carbon nanotubes were produced by the HiPCO® process and used as received without any further treatment (referred to as *p*-SWCNTs). The *p*-SWCNTs were dispersed in either *o*-DCB, *o*-xylene or diglyme by ultrasonication for 15 min under air exclusion. This SWCNT dispersion was then added to the solution of lithium pentynylide. During the reaction sequence the nucleophilic addition of the in situ generated lithium acetylide leads to the covalent attachment of the alkyne moiety to the SWCNT scaffold. This addition step is accompanied by the introduction of a negative charge to the SWCNT framework to yield intermediate species of the type $(\text{pentyne})_n$-SWCNT^{n-}. The resulting coulombic repulsion of the negatively charged SWCNTs leads to a debundling and an individualization of the aggregated tube material, as revealed by the formation of a homogeneous black dispersion. The subsequent reoxidation of the charged $(\text{pentyne})_n$-SWCNT^{n-} intermediates by air yields neutral $(\text{pentyne})_n$-SWCNT derivatives, which exhibit pronounced dispersibility in organic solvents such as THF or *o*-DCB.

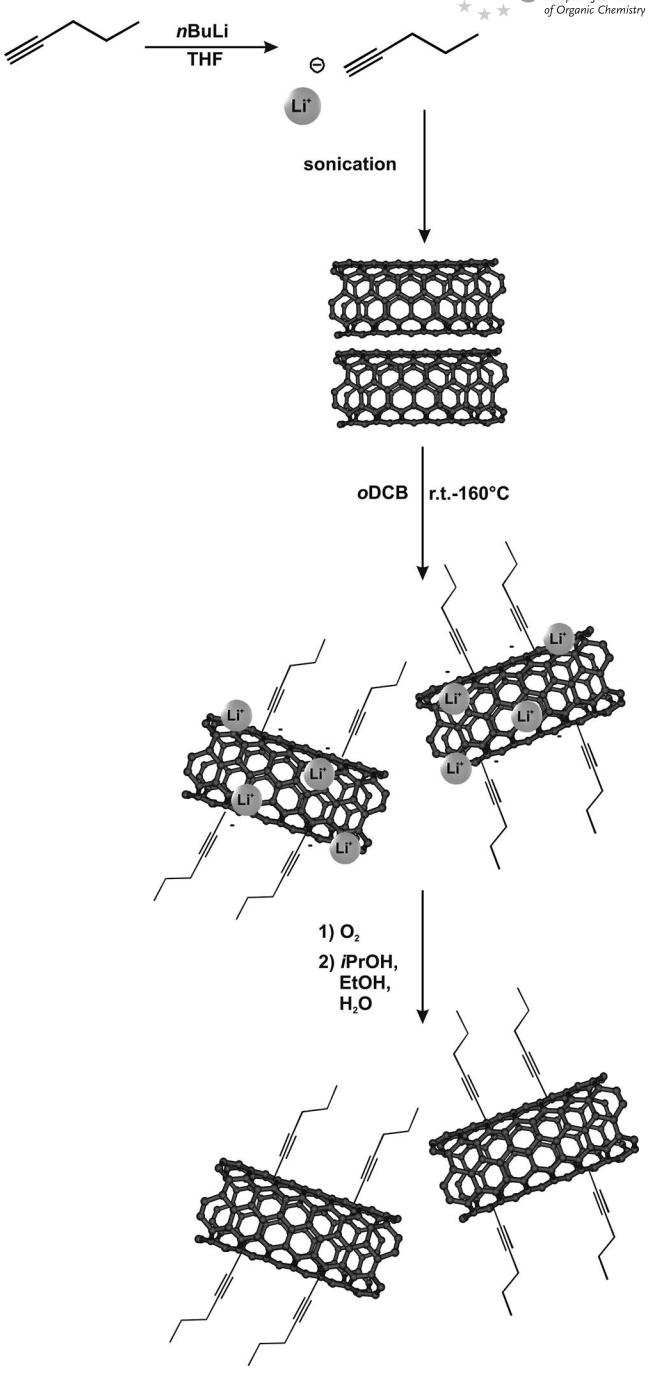

Scheme 1. Nucleophilic addition of lithium pentynylide to *p*-SWCNTs followed by reoxidation of the intermediately charged derivatives.

In contrast to the corresponding reactions with alkylides[21,36,37] or amides,[38] lithium acetylide based reaction sequences require elevated temperatures. Therefore, in this study a variety of different solvents, for example, *o*-DCB, *o*-xylene or diglyme, were investigated to open a larger temperature window due to the higher boiling points of these solvents. To investigate the influence of reaction temperature on the nucleophilic sidewall addition of lithium acetylides to SWCNTs, the reaction mixture was stirred while heating at different temperatures for 20 h.

This variation of reaction conditions allows the temperature and solvent parameters of the reaction sequence to be investigated and is the foundation for successful SWCNT functionalization with lithium acetylides, which is underlined by a detailed Raman spectroscopic study (Figure 1).

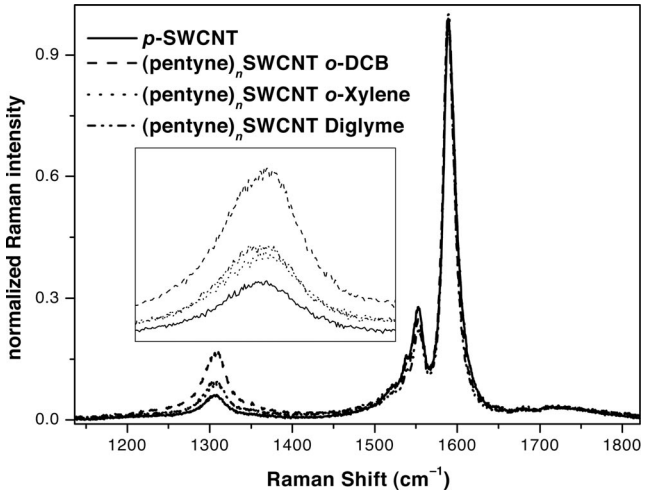

Figure 1. Raman spectra (D and G bands) of *p*-SWCNT (as received) and lithium pentynylide functionalized nanotubes [(pentyne)$_n$-SWCNT] in different solvents at 160 °C. Excitation wavelength = 633 nm.

The degree of functionalization can be estimated from the ratio of the D and G bands in the Raman spectra.[43] Whereas the G band, a graphitic sp^2 feature of carbon nanotubes, remains constant, the D band intensity increases in the case of covalent addition to the SWCNT sidewall as an sp^3 centre is generated in the carbon network. By comparing the degree of functionalization deduced from the corrected $(D/G)/(D_0/G_0)$ ratios in different solvents, the reaction in a THF/*o*-DCB mixture was found to give the highest degree of functionalization of the SWCNT material [at 160 °C and 633 nm, $(D/G)/(D_0/G_0) = 3.3$]. On the other hand, reaction sequences at a reaction temperature of 160 °C with solvents like *o*-xylene or diglyme lead to derivatized SWCNT samples with only a slight increase in D band intensity [1.5 (THF/*o*-xylene); 1.6 (diglyme)]. The reason for the higher degree of functionalization in the case of *o*-DCB is presumably based on the drastically increased dispersibility of SWCNTs in this halogenated solvent accompanied by a pronounced debundling and individualization of the tube material.

To exclude possible side-reactions of *o*-DCB with carbon nanotubes under ultrasonic treatment,[44] which yield a pronounced Raman D band signal, a blind test was carried out. For this purpose a *p*-SWCNT sample was treated under the same reaction conditions; however, no *n*-butyllithium was added to deprotonate the alkyne. As can be clearly seen in the Raman spectrum of the reference sample (*ref*-SWCNT; Figure 2), no increase in D band intensity or any other changes in the lineshape of the signals can be detected. In addition, the XPS spectra of the pentyne-derivatized SWCNT material [(pentyne)$_n$-SWCNT] and the reference sample of the blind test exhibit no Cl 2p core level signal (see the Supporting Information). This leads us to the conclusion that HiPCO® SWCNTs are not affected by *o*-DCB under the reaction conditions used for covalent sidewall functionalization with lithium acetylides.

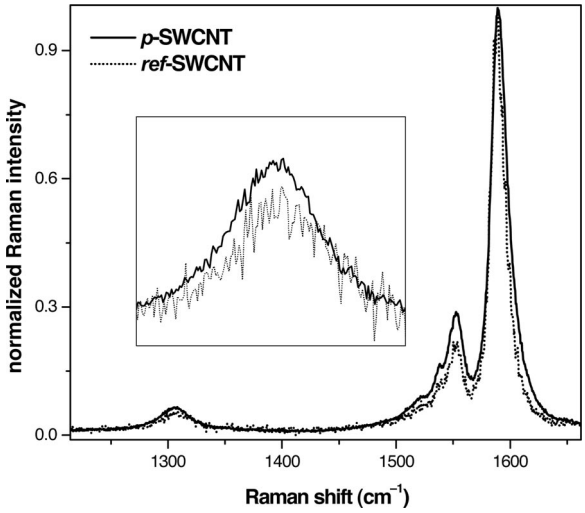

Figure 2. Raman spectra of *p*-SWCNT (as received) and *ref*-SWCNT (functionalization sequence without the addition of *n*BuLi) in *o*-DCB. Excitation wavelength = 633 nm.

To investigate the temperature dependence of the degree of functionalization, the reaction was carried out at 20, 80, 120 and 160 °C. As can be concluded from the increase in D band intensity observed in Figure 3, an elevated temperature leads to an increased degree of functionalization. Between room temperature and 80 °C no significant functionalization of the *p*-SWCNT starting material by lithium alkynylides is detectable. By raising the reaction temperature to 120 and 160 °C, however, the intensity of the D band increases considerably (Figure 3).

Further evidence for the covalent attachment of the pentyne moiety to the SWCNT scaffold was found by thermogravimetric analysis (TGA). The resulting mass/temperature profile of the (pentyne)$_n$-SWCNT sample, obtained at 120 °C, in the temperature range 100–700 °C clearly indicates an increased mass loss of 11% compared with the unfunctionalized starting material (*p*-SWCNT) as a result of the introduction of alkyne groups (Figure 4). In addition, a simultaneous mass spectrometric (MS) investigation of the cleaved volatile species allowed fragments of the pentyne substituent to be detected.

The detected fragments, which can clearly be assigned to the pentyne addend, are $CCCH_2CH_2CH_3$ (m/z = 67), $CH_2CH_2CH_3$ (m/z = 43) and $CCCH_2$ (m/z = 38). The appearance of these signals at temperatures between 350 and 550 °C also correlates with the temperature range in which maximum loss of mass of the sample is detected. The fact that this is the temperature range in which covalent C–C bonds are cleaved and the absence of any signals in the tem-

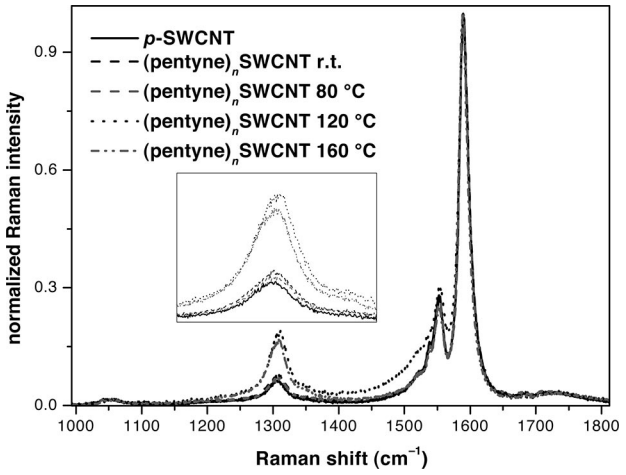

Figure 3. Raman spectra of different $(pentyne)_n$-SWCNT materials obtained by the functionalization of *p*-SWCNT (as received) with lithium pentynylide at different reaction temperatures. Excitation wavelength = 633 nm.

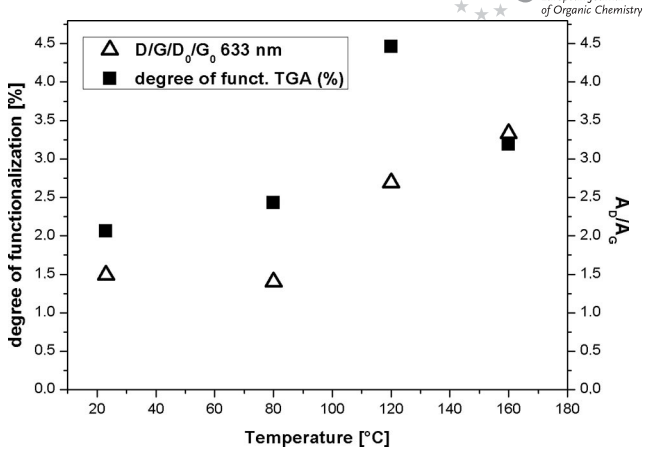

Figure 5. Degree of functionalization as a function of reaction temperature for different $(pentyne)_n$-SWCNT samples derived from TGA measurements as well as normalized Raman $(D/G)/(D_0/G_0)$ ratios.

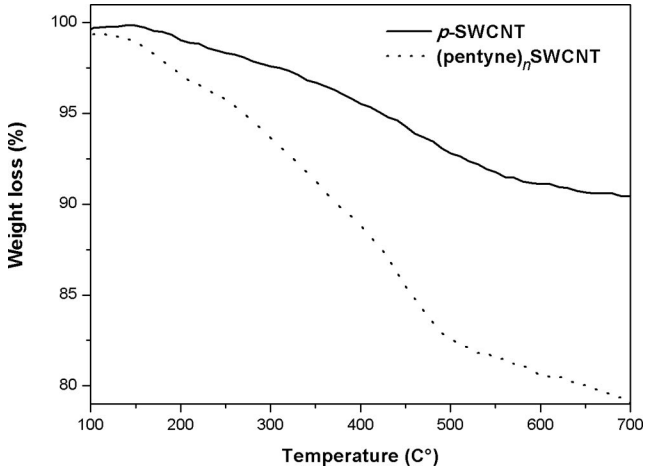

Figure 4. TGA weight loss from the starting material (*p*-SWCNT) and $(pentyne)_n$-SWCNTs (*o*-DCB, 120 °C).

perature range 150–250 °C (non-covalently attached species) substantiates the assumption of covalent bonding of the pentyne units to the sidewalls of the carbon nanotubes. This correlation between the observed temperature detachment profile and covalent SWCNT functionalization has also been reported by other groups.[45] The loss of mass calculated from the TGA data translates into a degree of functionalization of 4.5% (see the Supporting Information). On average, every 22nd carbon atom of the nanotube carries a pentyne addend.

Calculated degrees of functionalization based on Raman and TGA data as a function of reaction temperature are depicted in Figure 5. Both characterization methods independently confirm the formation of $(pentyne)_n$-SWCNT derivatives and also reflect the increasing degree of functionalization with elevated reaction temperature.

Owing to their highly increased dispersibility in organic solvents such as THF and *o*-DCB, the UV/Vis/NIR and fluorescence spectroscopic investigations of the derivatized materials could be carried out in homogeneous solution. As the starting SWCNT material (*p*-SWCNT) does not exhibit any dispersibility in THF at all, the corresponding optical spectra of the unfunctionalized SWCNTs were recorded in a surfactant-based solution of sodium dodecylbenzenesulfonate (SDBS)/D_2O (Figure 6 left) and *o*-DCB (Figure 6 right). The spectrum of *p*-SWCNT in SDBS/D_2O (left) exhibits absorption peaks characteristic of the transitions between the van Hove singularities in the density of states (DOS) of metallic (M) and semiconducting (S) nanotubes. The covalent attachment of functionalities to the SWCNT sidewall and the concomitant variation of the π-system by the generation of sp^3 defects usually leads to a broadening and reduction of van Hove singularities and an unstructured absorption spectrum in comparison to the unfunctionalized *p*-SWCNT material. Thus, the acquired spectrum of pentyne-functionalized SWCNTs [$(pentyne)_n$-SWCNT] in SDBS/D_2O exhibits less pronounced absorption signals. Nevertheless, the van Hove transitions are still present due to the functionalization-induced individualization of the SWCNT bundles and the comparably low defect density of the modified $(pentyne)_n$-SWCNT derivatives. Similar behaviour has been observed for alkylated and aminated carbon nanotubes.[38] Furthermore, a different line-shape profile, especially in the S_{11} (1100–1600 nm) and S_{22} (600–100 nm) region, can be detected, which is also typical for sidewall-functionalized carbon nanotubes.[46] The spectra on the right of Figure 6 represent the corresponding sample dissolved in *o*-DCB, as even unfunctionalized SWCNTs are quite dispersible in this solvent. Compared with the SDBS/D_2O spectra, the van Hove singularities of the *p*-SWCNTs in *o*-DCB exhibit lower intensities than the $(pentyne)_n$-SWCNTs due to a higher degree of bundling of the unfunctionalized material in organic solvents, clearly demonstrating the improved dispersibility of the pentyne-function-

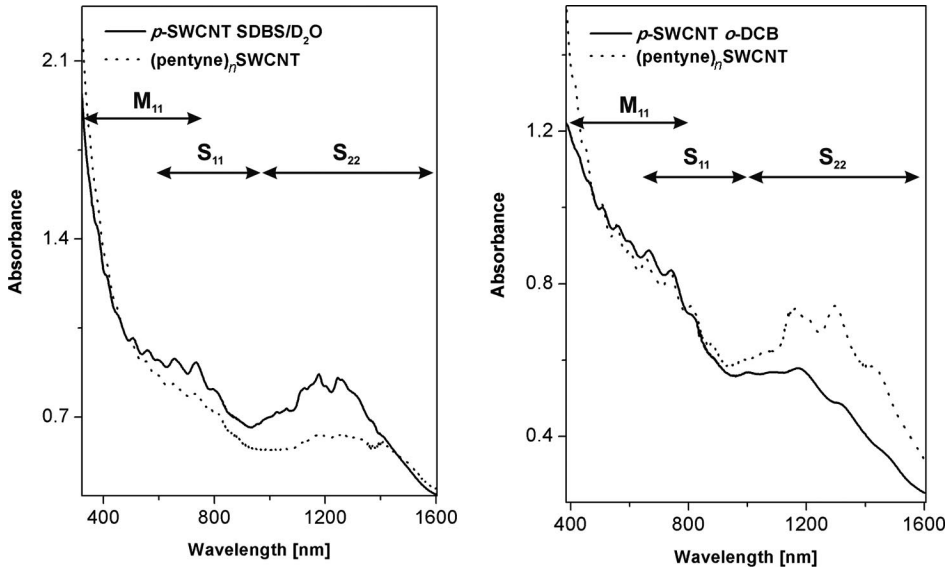

Figure 6. UV/Vis/NIR absorption spectra of *p*-SWCNT (as received) and (pentyne)$_n$-SWCNTs (*o*-DCB, 120 °C) in SDBS/D_2O (left) and *o*-DCB (right).

alized material due to the attachment of solubilizing substituents. In particular, the transitions in the semiconducting region (S_{11}) exhibit a more pronounced intensity in the case of (pentyne)$_n$-SWCNTs.

This observation is further supported by fluorescence spectroscopy. Fluorescence spectra were recorded from SDBS/D_2O dispersions at excitation wavelengths of 660 and 785 nm and normalized to the λ_{max} values at 6523 cm^{-1} (660 nm) and 6505 cm^{-1} (785 nm). In general a reduced emission intensity of the pentyne-derivatized SWCNT material relative to the unfunctionalized *p*-SWCNT sample can be observed (see the Supporting Information). This gives us an additional hint of a successful sidewall functionalization as SWCNT emission is very sensitive to the changes in the electronic states that occur on rehybridization of sp^2 carbon atoms to the sp^3 configuration.[37]

The correlation between reaction temperature, degree of functionalization and dispersibility can be demonstrated by a UV/Vis/NIR spectroscopic investigation of the (pentyne)$_n$-SWCNT derivatives obtained at different reaction temperatures (Figure 7). Equal amounts of different (pentyne)$_n$-SWCNT samples were dispersed in 3 mL of THF by ultrasonication for 30 min. The samples were subsequently centrifuged at 7000 r/min for 5 min to remove larger aggregates. As mentioned above, the nucleophilic addition of in situ generated lithium alkynylides is a temperature-dependent process. Thus, in the temperature regime between room temperature and 80 °C, no significant absorption was detected due to the low dispersibility of the derivatized material. In contrast, samples obtained at reaction temperatures of 120 and 180 °C exhibit an increased UV/Vis/NIR absorption in THF solution. This observation is in total agreement with the Raman data, which revealed a direct correlation between reaction temperature and degree of functionalization.

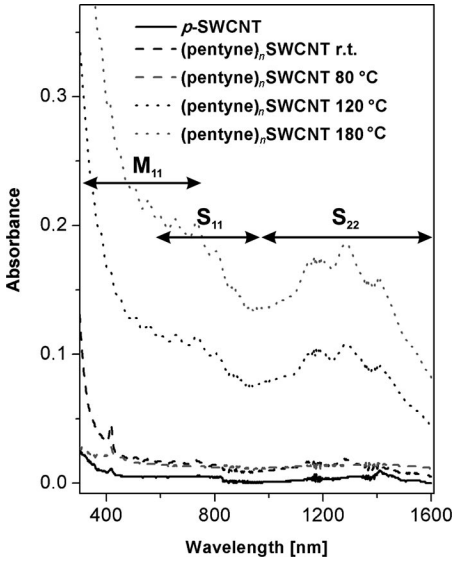

Figure 7. UV/Vis/NIR spectra of temperature-dependent functionalized (pentyne)$_n$-SWCNTs.

On the other hand, as less reactive species undergo reactions in a more selective manner, a higher addition selectivity of lithium alkynylides towards different SWCNT species, for example, metallic versus semiconducting, or of different size diameters as well chiralities, can be expected. To evaluate this rationale, a detailed analysis of the radial breathing-mode (RBM) region in the Raman spectra is required. The RBM region of the spectra recorded at an excitation wavelength of 633 nm, at which bands arising from both semiconducting and metallic tubes can be observed, indicates a decrease in Raman intensity for small-diameter semiconducting tubes due to their preferred functionalization (see

the Supporting Information). In general, the attachment of a functional moiety to the SWCNT sidewall and the resulting debundling due to the improved dispersibility of the functionalized SWCNT material is associated with a decrease or increase in the RBM intensities.[43,47] A detailed data analysis shows that there is a decrease in the RBM signal intensity especially in the high-frequency region, where small-diameter chiralities resonate at around 250–300 nm, and an increase in the RBM signal intensity in the low-frequency region (large diameters), which cannot be ascribed to debundling effects. For this reason the RBM region was normalized to a resonance signal at low reciprocal wavenumbers, in this case 193 cm^{-1} (633 nm excitation, Figure 8A), 185 cm^{-1} (532 nm excitation, Figure 8B) and 200 cm^{-1} (785 nm excitation, Figure 8C), at which the effect of change in intensity due to debundling and functionalization is low. The spectrum produced at an excitation wavelength of 633 nm (Figure 8A), at which both metallic and semiconducting tubes resonate, illustrates the general trend of decreasing RBM intensities for functionalized tubes at higher wavenumbers, being directly correlated to smaller-diameter SWCNTs. In the low-frequency RBM region (200–240 cm^{-1}), the intensities of the smaller metallic tubes (11,5) (12,3) and (13,1) show a decrease in intensity that is manifested in a step-by-step reduction of the RBM intensity towards smaller tube diameters (10,3), (9,4) and (7,5), reaching a maximum in the near disappearance of the smallest semiconducting tube chirality (8,4) and vanishing for (8,3). This inversely proportional relation between reactivity and diameter can be explained by the higher strain of small-diameter nanotubes and is in agreement with our previous results.[40,48,49] In addition, the normalized RBM signals at the excitation wavelengths of 532 and 785 nm show a decrease in RBM intensities, which is more pronounced with increasing wavenumber and results in the complete disappearance of the signals of the semiconducting (9,2) and (10,0) SWCNTs (Figure 8B). A distortion of these results due to the debundling effect would lead to an intensity increase especially of the metallic tubes (210–290 cm^{-1}) at an excitation wavelength of 532 nm and thus can be excluded, also in comparison with results observed with SDBS processed samples.[47] These results manifest the selectivity towards small-diameter nanotubes of this introduced reaction pathway, which we have also reported for the nucleophilic addition of *tert*-butylmagnesium chloride and for reductive alkylation reactions.[44]

To widen the scope of the nucleophilic addition of acetylides further, alkynylides with different topologies were used. For this reason the reaction sequence was also carried out with decyne (**2**) under the same reaction conditions. In this case a comparable increase in the ratio of D/G Raman bands was observed, which indicates a successful reaction of other linear terminal acetylides (see the Supporting Information).

In addition, we were also interested in the reactivity and selectivity of aromatic alkynylides. With this species, the in situ formed carbanions are stabilized by the corresponding aromatic ring system, and therefore a less pronounced reactivity and a more pronounced selectivity in comparison with their aliphatic analogues may be expected.

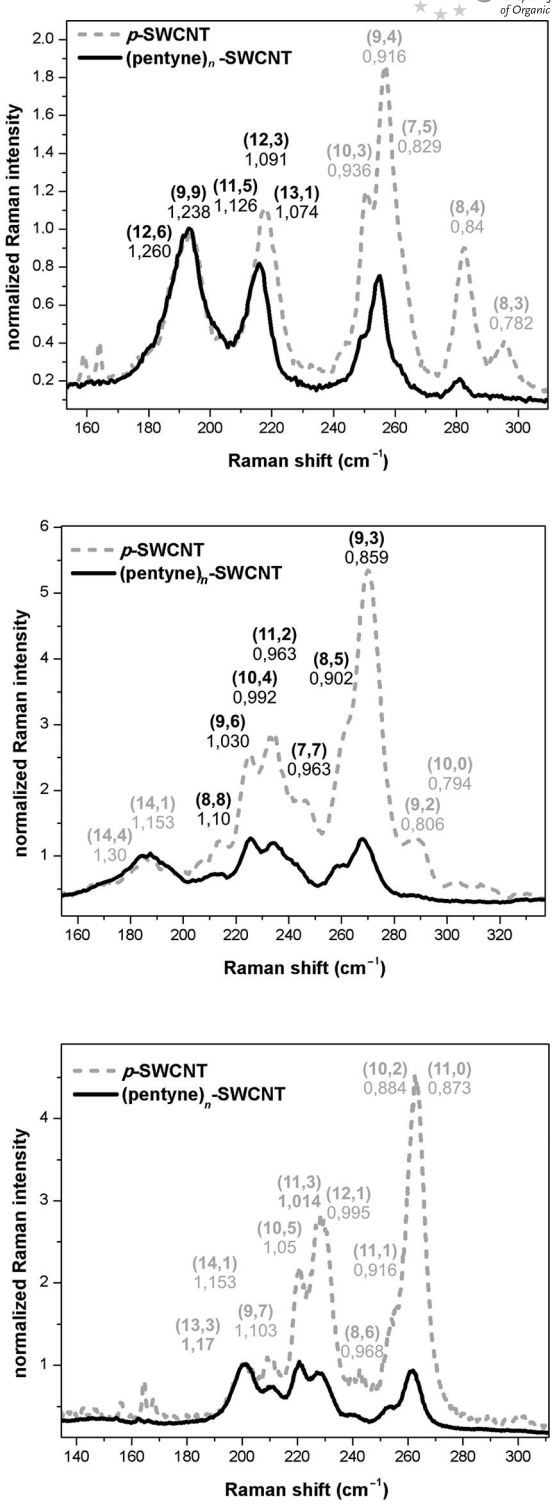

Figure 8. Normalized RBMs of *p*-SWCNT (as-received) and $(pentyne)_n$-SWCNT with related indices (metallic = black; semiconducting = grey) and diameters. Excitation wavelengths = 633 nm (A), 532 nm (B) and 785 nm (C).

This rationale is supported by ab initio calculations at the MP2 level of theory using the 6-311G* basis set.[42] In the deprotonated pentyne molecule a partial negative

charge (neutral atomic orbital populations) of –0.459 is located at the terminal sp C atom, whereas the terminal sp C atom of phenylacetylide exhibits a clearly decreased partial charge of –0.068 and, as a consequence, is a considerably weaker nucleophile.[50] For this reason a reduced reactivity in the nucleophilic addition to the tube sidewalls is expected. Unfortunately, the nucleophilic reactivity of the two aromatic stabilized acetylides, lithium phenylacetylide and lithium *m*-tolylacetylide, towards SWCNT sidewall addition is so low that almost no functionalization of the carbon nanotubes can be observed in Raman spectroscopic and TGA investigations (see the Supporting Information). Therefore aliphatic terminal lithium acetylides are the weakest nucleophiles that are capable of direct sidewall functionalization thus far.

Conclusions

Herein we present a reaction sequence for the functionalization of SWCNTs with lithium acetylides, less nucleophilic organometallic reagents than the previously reported lithium alkylides and amides. The successful covalent functionalization of SWCNTs with these in situ generated alkynylide functionalities in this reaction sequence has been proven by TGA/MS, Raman, fluorescence and UV/Vis/NIR spectroscopy. A detailed study of the nucleophilic addition sequence with variation of different reaction parameters such as solvent or temperature has been carried out, yielding more soluble SWCNT derivatives. We have demonstrated that the nucleophilic addition of in situ generated alkynylide ions is a temperature-dependent reaction, which has never been observed for SWCNTs up to now and therefore mirrors an input of activation energy, which has to be investigated in ongoing studies. The degree of functionalization [approximately 4.5% (pentyne, TGA)] of this protocol is comparable to other nucleophilic addition reactions involving organolithium reagents.[37,38] As expected, a detailed investigation of the RBM region of the Raman spectra confirms that the addition of alkynylide anions to carbon nanotubes is selective. In these studies, the addition reaction was found to preferentially take place on smaller-diameter SWCNTs. Selectivity in terms of metallic versus semiconducting SWCNTs could not be detected in this case. The clear evidence for successful functionalization with terminal aliphatic acetylides prompted us to investigate other in situ generated alkynylides. By comparing linear acetylides with their cyclic aromatic counterparts, the effect of stabilization of the formed carbanion by an aromatic π-system could be demonstrated. Based on this stabilization the reactivity of aromatic acetylides dropped to a level at which hardly any SWCNT sidewall functionalization could be detected.

Experimental Section

Materials: Single-walled carbon nanotubes (*p*-SWCNT) produced by the HiPCO® process were obtained from Unidym (Lot number P0355; grade: pure; TGA residue 5 wt.-%) and used as received without any further treatment. Chemicals and solvents were purchased from Acros (Geel, Belgium) and Merck KGaA (Darmstadt, Germany) and were also used as received.

Acetylide-Functionalized SWCNTs [(alkyne)$_n$-SWCNTs]: In a heat-dried and nitrogen-purged four-necked round-bottomed flask (250 mL) equipped with two gas inlets and pressure compensation, the corresponding alkyne (pentyne, decyne, phenylacetylene, *m*-tolylacetylene; 10.4 mmol) was dissolved in dry THF. The solution was cooled to 0 °C, and *n*-butyllithium (0.9 equiv.) was added dropwise over a period of 10 min. The solution was stirred at room temperature for 1 h. In a 250 mL nitrogen-purged and heat-dried three-necked round-bottomed flask equipped with two gas inlets, HiPCO SWCNTs (5 mg) were dispersed in anhydrous THF (100 mL) by ultrasonication for 30 min. This dispersion was transferred under an inert gas to the first flask. A stable black solution was produced, which was stirred at room temperature for 20 h and subsequently quenched by bubbling oxygen through the solution for 30 min. The dispersion was diluted with cyclohexane (100 mL), transferred to a separation funnel and purged with water (250 mL). The organic layer with the nanotubes was filtered through a 0.2 μm reinforced cellulose membrane filter (Sartorius) and thoroughly washed with THF, 2-propanol, ethanol and water (250 mL each). The resulting black solid was dried in a vacuum oven at 75 °C overnight. In the case of the other alkynes (decyne, phenylacetylene, *m*-tolylacetylene), the reaction sequence was performed in different solvents (*o*-DCB, *o*-xylene, diglyme) at elevated temperatures (80, 120, 160 °C).

Instruments and Measurements: Raman spectra were obtained with a Horiba Jobin Yvon LabRAM Aramis spectrometer (excitation at 532, 633 and 785 nm). Thermogravimetric analysis (TGA) was performed with a Netzsch STA 409 CD instrument equipped with a Skimmer QMS 422 mass spectrometer (MS/EI) with the following programmed time-dependent temperature course: 24–100 °C at 10 °C/min, 100 °C for 1 h, 100–700 °C at 10 °C/min, 700 °C for 1 h and cooling to 24 °C. The initial sample weights were 5–10 mg, and the whole experiment was accomplished under He as the inert gas with a gas flow of 80 mL/min. UV/Vis/NIR spectra were obtained with a Shimadzu UV-3102pc spectrometer. Fluorescence spectra were obtained with an NS1 NanoSpectralyzer (excitation at 660 and 785 nm) from Applied NanoFluorescence, LLC. Ultrasonications were performed with a Branson 2510-DTH Ultrasonic Processor. The solubilization of the as-received HiPCO material for the blind test was achieved by using a 1% solution of sodium dodecylbenzenesulfonate (SDBS; Acros) in deuterium oxide and *o*-DCB. The ultrasonication time was 30 min. The spectra were measured from the supernatant after precipitation (1 d) of the insoluble SWCNTs. X-ray induced photoelectron spectra were measured on bucky paper of the respective material. A monochromatized Al-K_α small-spot X-ray source ($\eta\omega$ = 1486.6 eV) was used as the photon source. All binding energies refer to the Fermi level, which was regularly calibrated using the Au 4f core level at 84.00 eV.

Supporting Information (see footnote on the first page of this article): Raman spectra at all three excitation wavelengths, XPS core level spectra, TGA/MS profiles.

Acknowledgments

This work was supported by the Deutsche Forschungsgemeinschaft (DFG) and the Cluster of Excellence "Engineering of Advanced Materials". Furthermore, we thank the Interdisciplinary Center for Molecular Materials (ICMM) for financial support.

[1] S. Iijima, *Nature* **1991**, *354*, 56–58.
[2] J. N. Coleman, U. Khan, W. J. Blau, Y. K. Gun'ko, *Carbon* **2006**, *44*, 1624–1652.
[3] M. Iurlo, D. Paolucci, M. Marcaccio, F. Paolucci, *Chem. Commun.* **2008**, 4867–4874.
[4] A. Hirsch, *Angew. Chem. Int. Ed.* **2002**, *41*, 1853–1859.
[5] A. Hirsch, O. Vostrowsky, *Top. Curr. Chem.* **2005**, *245*, 193–237.
[6] D. Tasis, N. Tagmatarchis, A. Bianco, M. Prato, *Chem. Rev.* **2006**, *106*, 1105–1136.
[7] K. D. Ausman, R. Piner, O. Lourie, R. S. Ruoff, M. Korobov, *J. Phys. Chem. B* **2000**, *104*, 8911–8915.
[8] J. L. Bahr, E. T. Mickelson, M. J. Bronikowski, R. E. Smalley, J. M. Tour, *Chem. Commun.* **2001**, 193–194.
[9] R. H. Baughman, A. A. Zakhidov, W. A. de Heer, *Science* **2002**, *297*, 787–792.
[10] S. Banerjee, T. Hemraj-Benny, S. S. Wong, *J. Nanosci. Nanotechnol.* **2005**, *5*, 841–855.
[11] F. Buffa, H. Hu, D. E. Resasco, *Macromolecules* **2005**, *38*, 8258–8263.
[12] A. Hamwi, H. Alvergnat, S. Bonnamy, F. Beguin, *Carbon* **1997**, *35*, 723–728.
[13] E. T. Mickelson, C. B. Huffman, A. G. Rinzler, R. E. Smalley, R. H. Hauge, J. L. Margrave, *Chem. Phys. Lett.* **1998**, *296*, 188–194.
[14] H. Touhara, F. Okino, *Carbon* **2000**, *38*, 241–267.
[15] T. Hemraj-Benny, S. S. Wong, *Chem. Mater.* **2006**, *18*, 4827–4839.
[16] W. Zhang, T. M. Swager, *J. Am. Chem. Soc.* **2007**, *129*, 7714–7715.
[17] V. Georgakilas, K. Kordatos, M. Prato, D. M. Guldi, M. Holzinger, A. Hirsch, *J. Am. Chem. Soc.* **2002**, *124*, 760–761.
[18] F. Mercuri, A. Sgamellotti, *Phys. Chem. Chem. Phys.* **2009**, *11*, 563–567.
[19] A. Penicaud, P. Poulin, A. Derre, E. Anglaret, P. Petit, *J. Am. Chem. Soc.* **2005**, *127*, 8–9.
[20] W. E. Billups, F. Liang, J. Chattopadhyay, J. M. Beach, *ECS Trans.* **2007**, *2*, 65–76.
[21] D. Wunderlich, F. Hauke, A. Hirsch, *J. Mater. Chem.* **2008**, *18*, 1493–1497.
[22] N. Tagmatarchis, V. Georgakilas, M. Prato, H. Shinohara, *Chem. Commun.* **2002**, 2010–2011.
[23] J. L. Bahr, J. M. Tour, *Chem. Mater.* **2001**, *13*, 3823–3824.
[24] J. L. Bahr, J. Yang, D. V. Kosynkin, M. J. Bronikowski, R. E. Smalley, J. M. Tour, *J. Am. Chem. Soc.* **2001**, *123*, 6536–6542.
[25] M. S. Strano, C. A. Dyke, M. L. Usrey, P. W. Barone, M. J. Allen, H. Shan, C. Kittrell, R. H. Hauge, J. M. Tour, R. E. Smalley, *Science* **2003**, *301*, 1519–1522.
[26] J. J. Stephenson, J. L. Hudson, S. Azad, J. M. Tour, *Chem. Mater.* **2006**, *18*, 374–377.
[27] M. Holzinger, O. Vostrowsky, A. Hirsch, F. Hennrich, M. Kappes, R. Weiss, F. Jellen, *Angew. Chem. Int. Ed.* **2001**, *40*, 4002–4005.
[28] H. Peng, P. Reverdy, V. N. Khabashesku, J. L. Margrave, *Chem. Commun.* **2003**, 362–363.
[29] P. Umek, J. W. Seo, K. Hernadi, A. Mrzel, P. Pechy, D. D. Mihailovic, L. Forro, *Chem. Mater.* **2003**, *15*, 4751–4755.
[30] Y. Ying, R. K. Saini, F. Liang, A. K. Sadana, W. E. Billups, *Org. Lett.* **2003**, *5*, 1471–1473.
[31] H. Peng, L. B. Alemany, J. L. Margrave, V. N. Khabashesku, *J. Am. Chem. Soc.* **2003**, *125*, 15174–15182.
[32] T. Nakamura, M. Ishihara, T. Ohana, A. Tanaka, Y. Koga, *Chem. Commun.* **2004**, 1336–1337.
[33] G. Viswanathan, N. Chakrapani, H. Yang, B. Wei, H. Chung, K. Cho, Y. Ryu Chang, M. Ajayan Pulickel, *J. Am. Chem. Soc.* **2003**, *125*, 9258–9259.
[34] R. Blake, Y. K. Gun'ko, J. Coleman, M. Cadek, A. Fonseca, J. B. Nagy, W. J. Blau, *J. Am. Chem. Soc.* **2004**, *126*, 10226–10227.
[35] S. Chen, W. Shen, G. Wu, D. Chen, M. Jiang, *Chem. Phys. Lett.* **2005**, *402*, 312–317.
[36] R. Graupner, J. Abraham, D. Wunderlich, A. Vencelova, P. Lauffer, J. Roehrl, M. Hundhausen, L. Ley, A. Hirsch, *J. Am. Chem. Soc.* **2006**, *128*, 6683–6689.
[37] D. Wunderlich, F. Hauke, A. Hirsch, *Chem. Eur. J.* **2008**, *14*, 1607–1614.
[38] Z. Syrgiannis, F. Hauke, J. Röhrl, M. Hundhausen, R. Graupner, Y. Elemes, A. Hirsch, *Eur. J. Org. Chem.* **2008**, 2544–2550.
[39] M. Mueller, J. Maultzsch, D. Wunderlich, A. Hirsch, C. Thomsen, *Phys. Status Solidi RRL* **2007**, *1*, 144–146.
[40] M. Mueller, J. Maultzsch, D. Wunderlich, A. Hirsch, C. Thomsen, *Phys. Status Solidi B* **2007**, *244*, 4056–4059.
[41] M. S. Strano, *J. Am. Chem. Soc.* **2003**, *125*, 16148–16153.
[42] N. Nair, W.-J. Kim, M. L. Usrey, M. S. Strano, *J. Am. Chem. Soc.* **2007**, *129*, 3946–3954.
[43] R. Graupner, *J. Raman Spectrosc.* **2007**, *38*, 673–683.
[44] K. R. Moonoosawmy, P. Kruse, *J. Am. Chem. Soc.* **2008**, *130*, 13417–13424.
[45] T. Umeyama, N. Tezuka, M. Fujita, Y. Matano, N. Takeda, K. Murakoshi, K. Yoshida, S. Isoda, H. Imahori, *J. Phys. Chem. C* **2007**, *111*, 9734–9741.
[46] D. Yoon, S.-J. Kang, J.-B. Choi, Y.-J. Kim, S. Baik, *J. Nanosci. Nanotechnol.* **2007**, *7*, 3727–3730.
[47] L. M. Ericson, P. E. Pehrsson, *J. Phys. Chem. B* **2005**, *109*, 20276–20280.
[48] A. Pekker, D. Wunderlich, K. Kamaras, A. Hirsch, *Phys. Status Solidi B* **2008**, *245*, 1954–1956.
[49] M. Mueller, J. Maultzsch, D. Wunderlich, A. Hirsch, C. Thomsen, *Phys. Status Solidi B* **2008**, *245*, 1957–1960.
[50] P. Karafiloglou, J.-P. Launay, *Chem. Phys.* **2003**, *289*, 231–242.

Received: July 27, 2009
Published Online: January 29, 2010

